Supporting Material

Amyloid Fibrillation of Insulin under Water-limiting Condition

Tae Su Choi[†], Jong Wha Lee[†], Kyeong Sik Jin[‡], and Hugh I. Kim[†,§*]

[†]Department of Chemistry, [‡]Pohang Accelerator Laboratory, and [§]Division of Advanced Materials Science, Pohang University of Science and Technology (POSTECH), Pohang 790-784, Republic of Korea

*Correspondence: hughkim@postech.edu

METHOD

Intrinsic Tyrosine Fluorescence

Intrinsic tyrosine fluorescence was monitored during the thermal denaturation of insulin using an excitation wavelength of 275 nm with the emission wavelength varying from 280 to 380 nm. The cuvette temperature was increased from 5 to 95 °C with a scan rate of 1.5 °C/min. The concentration of insulin was adjusted to 0.036 mg/mL. All solutions for fluorescence measurements contained 50 mM of imidazole–HCl buffer, and the pH value was adjusted to 7.0. Because imidazole buffer solutions show fluorescent properties at an excitation wavelength of 275 nm, blank solutions were measured to subtract the matrix effect.

DSC Peak Fitting

Peak fitting of the DSC thermograms was performed using the Gaussian distribution. The centers of each transition curve were estimated from the intrinsic tyrosine fluorescence of insulin. The mid-temperature value of each linear segment in the fluorescence data was selected as the initial T_0 of the transition curves, and multiple Gaussian curves were optimized to fit the overall shape of the DSC thermograms with an R^2 value of 0.998. The Gaussian distribution parameters for peak fitting are available in Table S3. All data for tyrosine fluorescence are available in the Supporting Material.

RESULT AND DISCUSSION

Intrinsic Tyrosine Fluorescence of Insulin during Thermal Denaturation

In order to obtain information about the intermediate species in the DSC thermograms, The intrinsic tyrosine fluorescence of insulin is further studied using fluorescence phase plots (Fig. S9-S12) at 302 nm (tyrosine) and 330 nm (tyrosinate).(1) In the absence of a structural change with respect to the tyrosine residues, the fluorescence intensity of tyrosine exhibits a linear relationship with the fluorescence intensity of tyrosinate as the temperature of the insulin solution increases; a change in the slope of a linear segment implies the occurrence of a structural conversion in insulin, which is related to the tyrosine residues. All solutions, except for those containing DMF, exhibit a transition segment that is similar to the temperature range of the thermal transition in DSC. These results indicate that the intermediate species share a structural feature related to the tyrosine residues

during the thermal transition of insulin. For the DMF systems, at least three segments are observed in the temperature range of the thermal transition in the DSC measurements (Fig. S9d and S9g). It has been reported that DMF induces a polypeptide chain in the random coil state to form an α-helical structure,(2) and also that DMF denatures the tertiary structure of the protein.(3) Presumably, the results obtained from the DMF solution are correlated to the sequential transition of the tertiary and secondary structure of insulin.

FIGURE S1. χ^2-R_g diagram from the pool of insulin conformation. The pair of experimental R_g value and corresponding χ^2 value is marked in red dash lines.

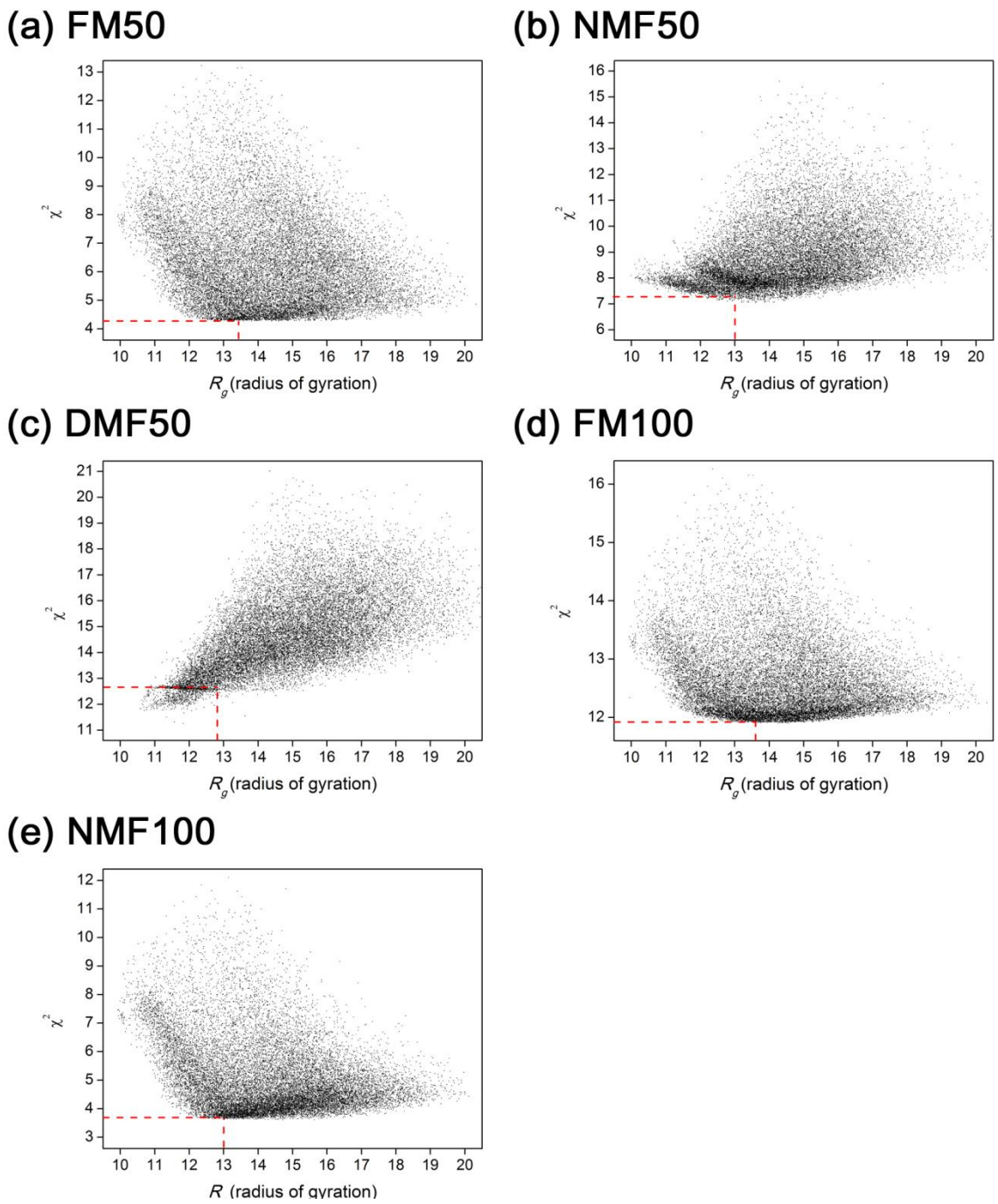

FIGURE S2. MALDI spectra of insulin in each solvent system. $[Insulin+H]^+$ is observed at *m*/*z* 5806.8.

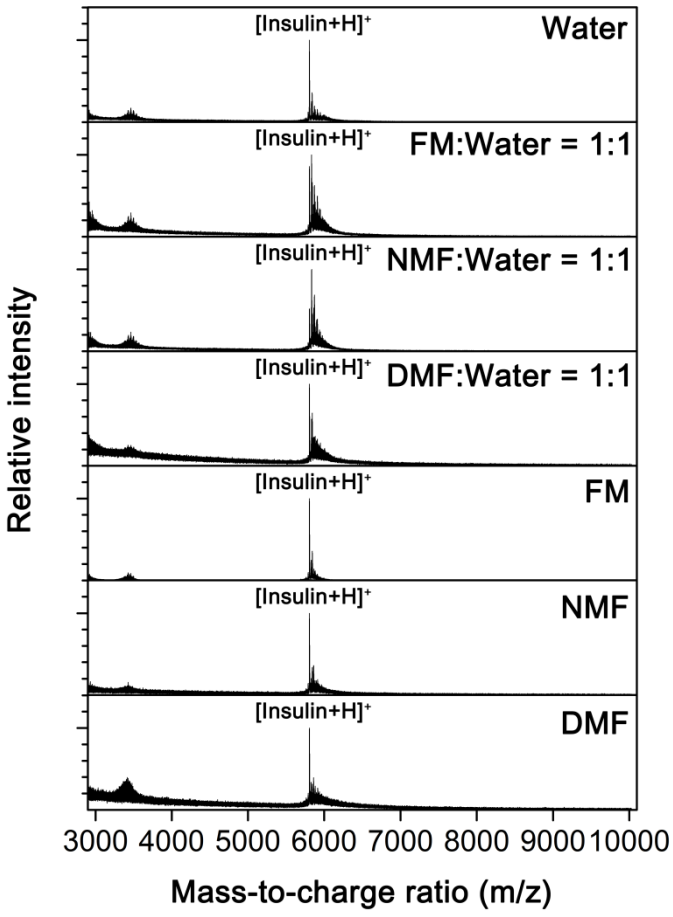

FIGURE S3. (a) Additional MD structures in FM50. Insulin chains A and B are marked in purple and cornflower blue. The secondary structure of residues B11–B17 is illustrated in red. (b) Pair-distance distribution function, $p(r)$, of insulin from experimental scattering curve and MD structures. (c) CRYSOL fitting results between experimental and theoretical scattering profiles for evaluating χ^2.

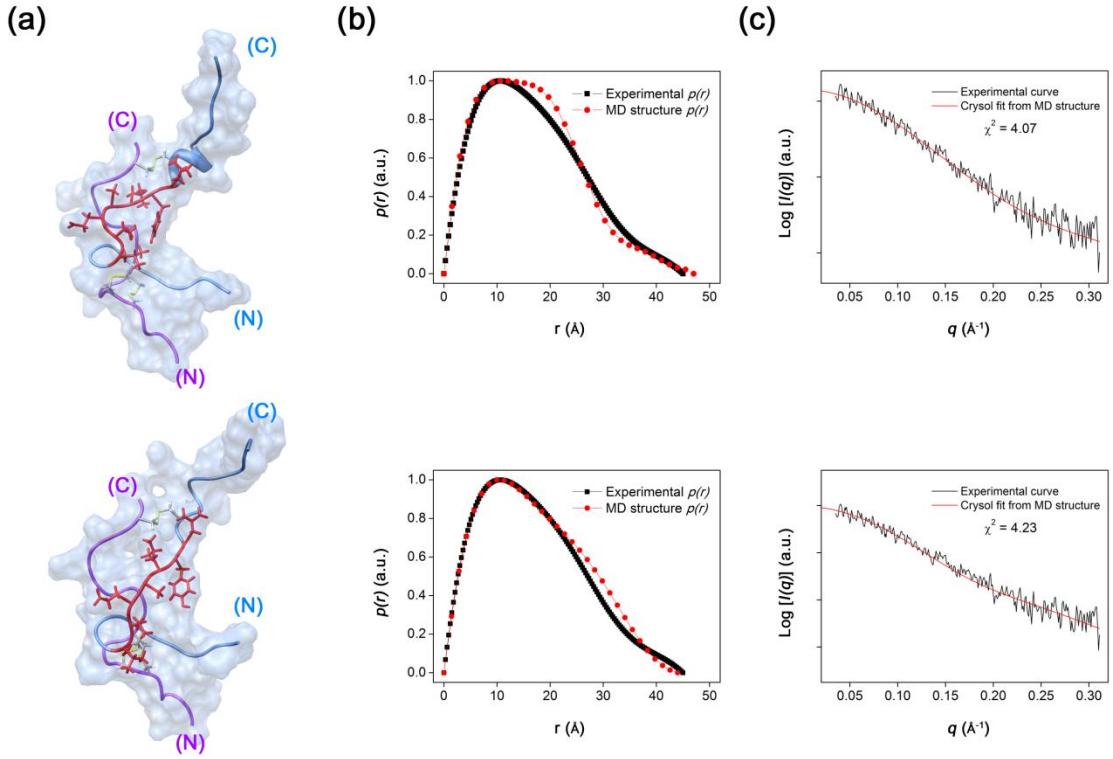

FIGURE S4. (a) Additional MD structures in NMF50. Insulin chains A and B are marked in purple and cornflower blue. The secondary structure of residues B11–B17 is illustrated in red. (b) Pair-distance distribution function, $p(r)$, of insulin from experimental scattering curve and MD structures. (c) CRYSOL fitting results between experimental and theoretical scattering profiles for evaluating χ^2.

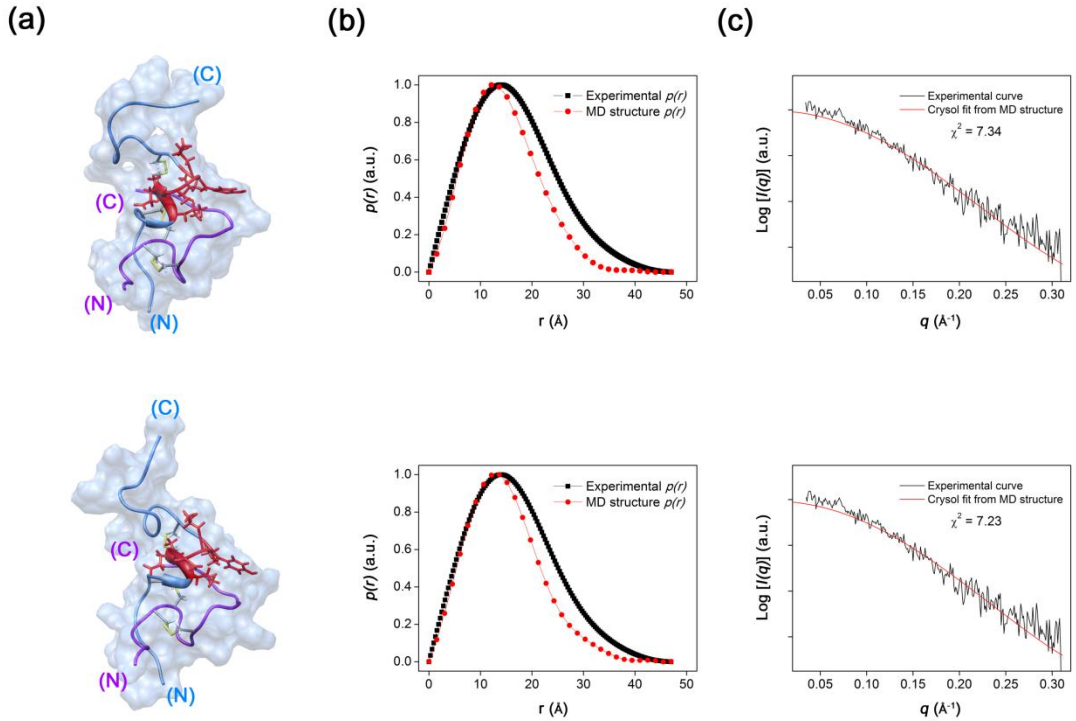

FIGURE S5. (a) Additional MD structures in DMF50. Insulin chains A and B are marked in purple and cornflower blue. The secondary structure of residues B11–B17 is illustrated in red. (b) Pair-distance distribution function, $p(r)$, of insulin from experimental scattering curve and MD structures. (c) CRYSOL fitting results between experimental and theoretical scattering profiles for evaluating χ^2.

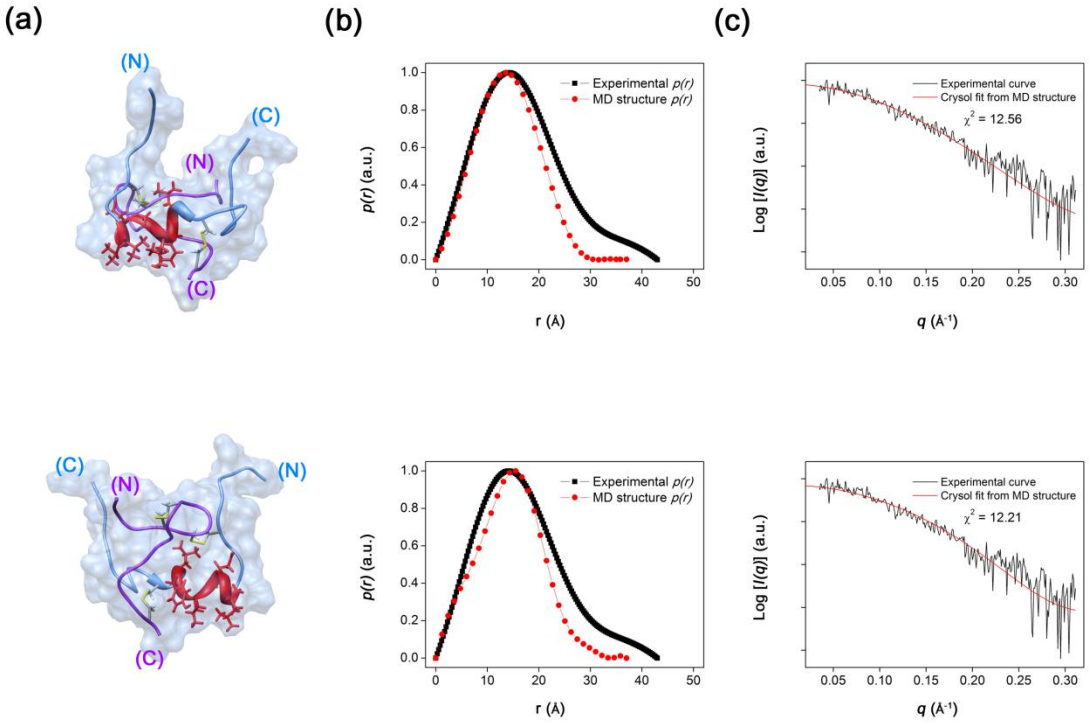

FIGURE S6. (a) Additional MD structures in FM100. Insulin chains A and B are marked in purple and cornflower blue. The secondary structure of residues B11–B17 is illustrated in red. (b) Pair-distance distribution function, $p(r)$, of insulin from experimental scattering curve and MD structures. (c) CRYSOL fitting results between experimental and theoretical scattering profiles for evaluating χ^2.

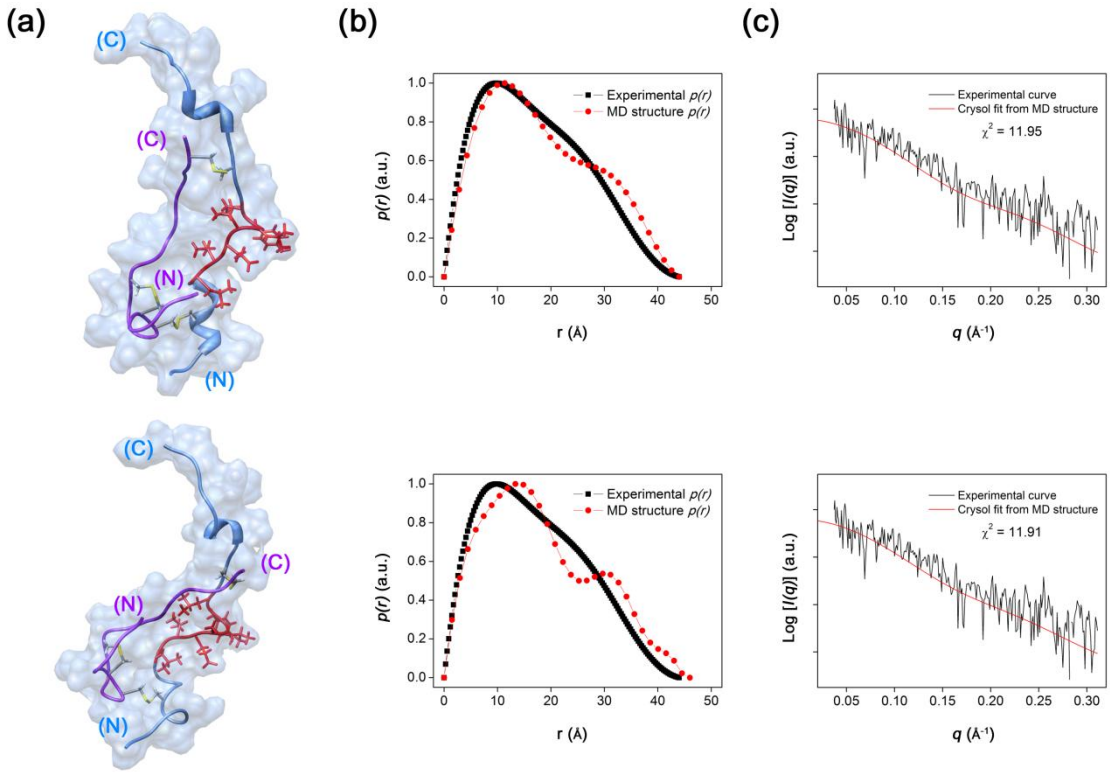

FIGURE S7. (a) Additional MD structures in NMF100. Insulin chains A and B are marked in purple and cornflower blue. The secondary structure of residues B11–B17 is illustrated in red. (b) Pair-distance distribution function, $p(r)$, of insulin from experimental scattering curve and MD structures. (c) CRYSOL fitting results between experimental and theoretical scattering profiles for evaluating χ^2.

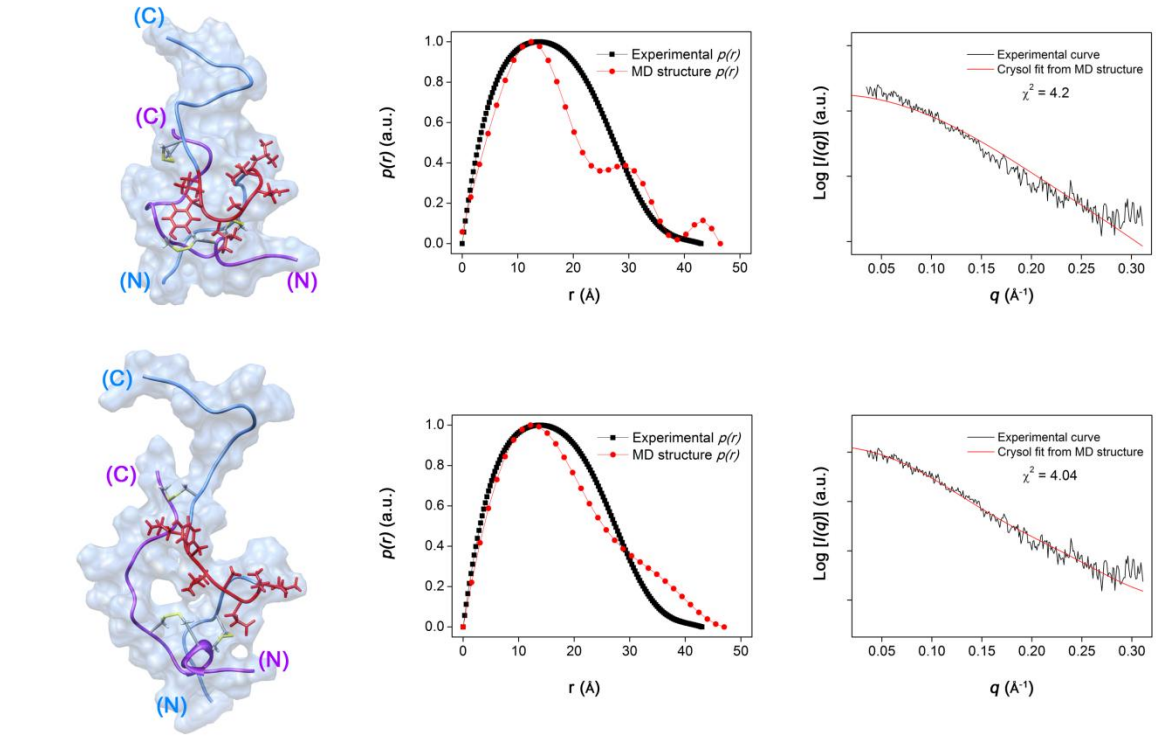

FIGURE S8. DSC thermograms of insulin in (a) binary mixtures and (b) organic solvents Thermogram of insulin in water is inserted as the control.

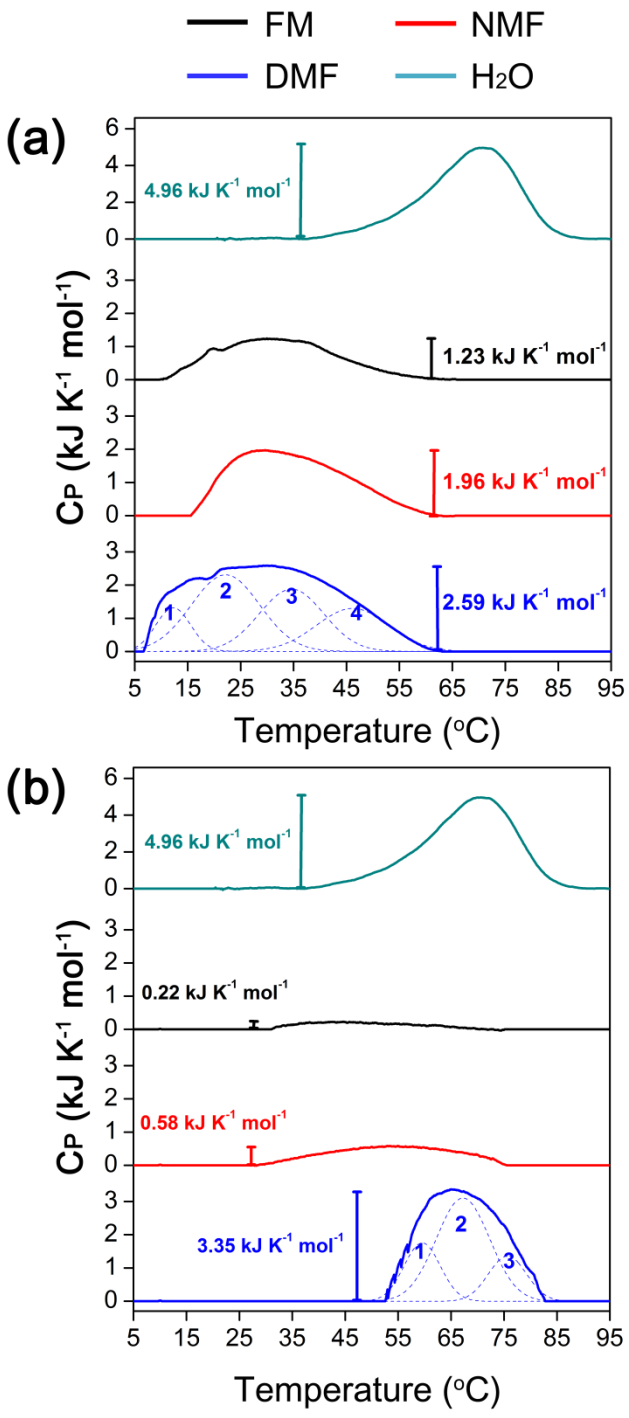

TABLE S1. Increase rates of R_g of insulin in various solvent conditions compared to crystal structure of monomeric insulin (PDB code: 3E7Y).

	R_g (Å)	R_X/R_{PDB}	Increase rate%
PDB code:3E7Y	11.6	1	+0%
FM50	13.6	1.17	+17%
NMF50	12.8	1.10	+10%
DMF50	12.6	1.08	+8%
FM100	13.9	1.19	+19%
NMF100	12.8	1.10	+10%

TABLE S2. Solvent accessible area (SAS) of residues B11-B17 in the simulated structures. Numbers in parentheses indicate the number of amino acid residues with α-helical structure.

	SAS of Residues B11-B17
PDB code: 3E7Y	4.9 nm^2 (7)
FM50	6.8 ± 1.2 nm^2 (0)
NMF50	5.3 ± 0.2 nm^2 (3)
DMF50	5.1 ± 0.5 nm^2 (7)
FM100	7.1 ± 0.6 nm^2 (0)
NMF100	8.8 ± 0.6 nm^2 (0)

TABLE S3. Gaussian distribution parameters for pick fitting of the DSC thermograms in Figure S8. *A*, μ, and σ respectively indicate amplitude, the center, and full width half-maximum for Gaussian function stated below, and Φ (kJ·mol^{-1}) indicates the area under the curve.

$$y = A \cdot e^{-\frac{1}{2}\left(\frac{x-\mu}{\sigma}\right)^2}$$

	Water : DMF = 1:1				DMF only			
	A	μ	σ	Φ	*A*	μ	σ	Φ
Peak 1	0.036	12.3	7.73	10.3	0.049	59.5	8.06	14.8
Peak 2	0.065	22.2	15.2	36.1	0.087	67.2	11.9	38.9
Peak 3	0.052	34.6	14.3	27.7	0.039	75.6	8.56	12.6
Peak 4	0.036	46.2	16.2	21.6				

FIGURE S9. Fluorescence phase plot of insulin in (a) water, (b) FM50, (c) NMF50, (d) DMF50, (e) FM100, (f) NMF100, (g) DMF100.

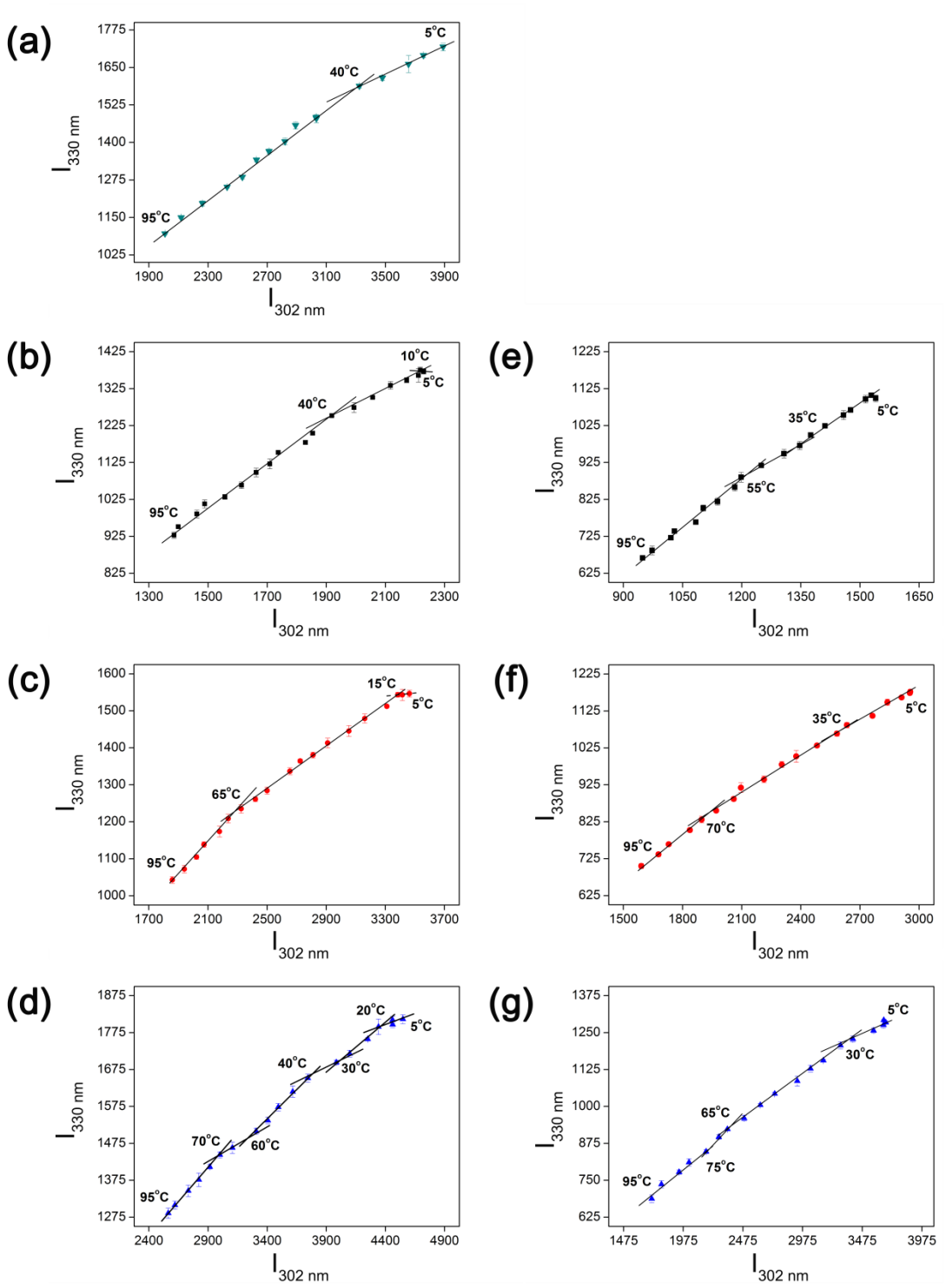

FIGURE S10. Fluorescence emission spectra of tyrosine during the thermal denaturation of insulin in water.

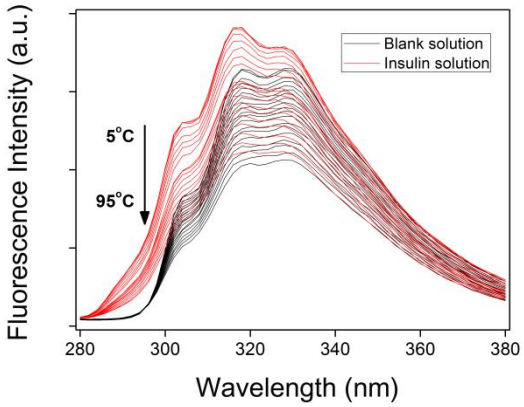

FIGURE S11. Fluorescence emission spectra of tyrosine during the thermal denaturation of insulin in (a) FM50, (b) NMF50, and (c) DMF50.

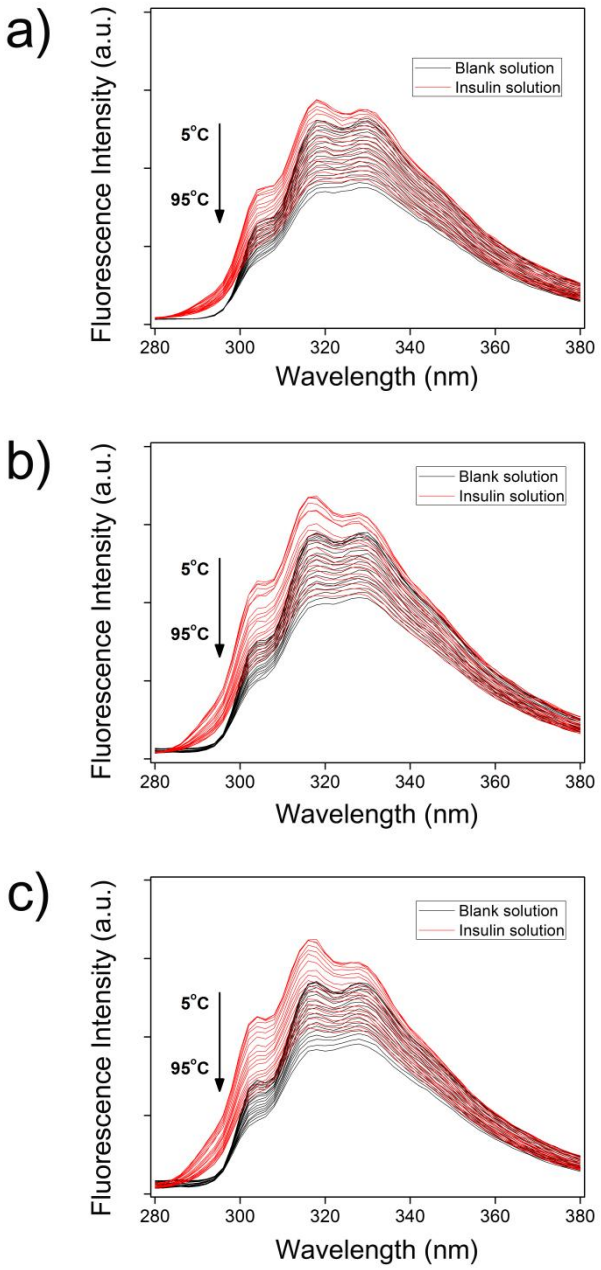

FIGURE S12. Fluorescence emission spectra of tyrosine during the thermal denaturation of insulin in (a) FM100, (b) NMF100, and (c) DMF100.

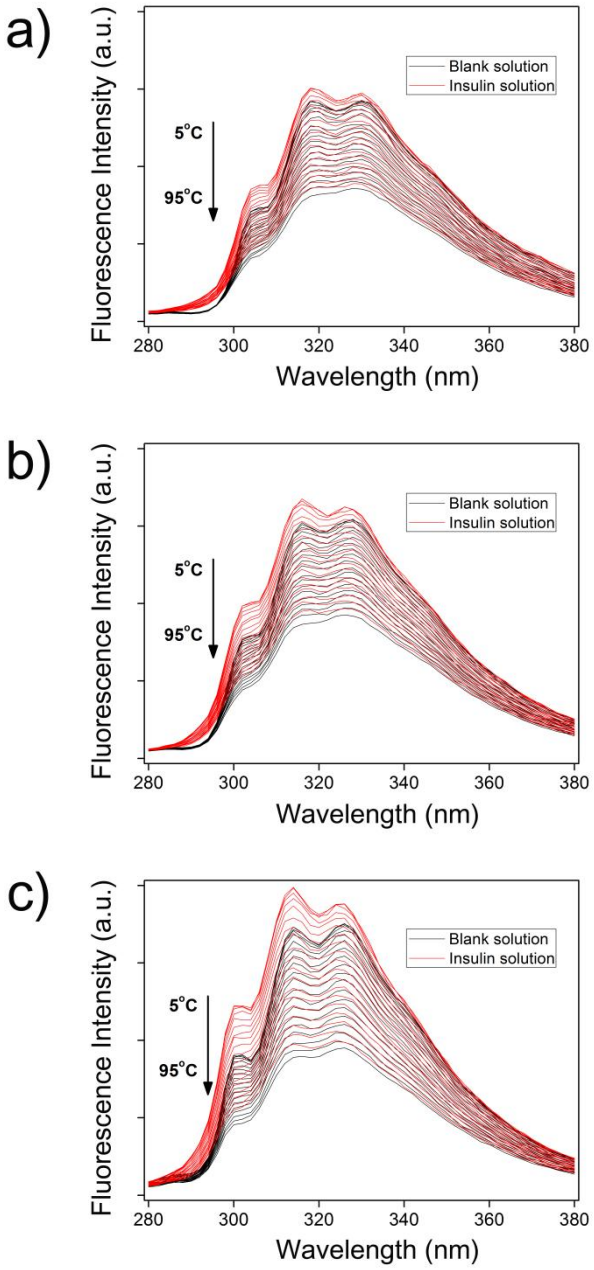

SUPPORTING REFERENCES

1. Bekard, I. B., and D. E. Dunstan. 2009. Tyrosine Autofluorescence as a Measure of Bovine Insulin Fibrillation. *Biophys. J.* 97:2521-2531.
2. Duhamel, J., S. Kanagalingam, …, M. W. Ingratta. 2003. Side-chain dynamics of an α-helical polypeptide monitored by fluorescence. *J. Am. Chem. Soc.* 125:12810-12822.
3. Herskovits, T. T., C. F. Behrens, …, E. R. Pandolfelli. 1977. Solvent denaturation of globular proteins Unfolding by the monoalkyl- and dialkyl-substituted formamides and ureas. *Biochim. Biophys. Acta*. 490:192-199.